

Formation Regularities of Grain-Boundary Interlayers of the α -Ti Phase in Binary Titanium Alloys

A. S. Gornakova^{a, *}, S. I. Prokofiev^{a, **}, K. I. Kolesnikova^{b, ***}, and B. B. Straumal^{a, ****}

^a*Institute of Solid-State Physics, Russian Academy of Sciences,
Ac. Ossipyan str. 2, Chernogolovka, 142432 Russia*

^b*National University of Science and Technology “MISIS”, Leninskii pr. 4, Moscow, 119049 Russia*

**e-mail: alenahas@issp.ac.ru*

***e-mail: prokof@issp.ac.ru*

****e-mail: kolesnikova@misis.ru*

*****e-mail: straumal@issp.ac.ru*

Received July 28, 2014; accepted August 20, 2015

Abstract—The microstructure of polycrystalline alloys of titanium with chromium (2, 4, and 5.5 wt %), cobalt (2 and 4 wt %), and copper (2 and 3 wt %) is investigated. Series of prolonged isothermal annealing of these materials are performed in a temperature range from 600 to 850°C (in vacuum). Annealing temperatures fall in two-phase regions $\alpha(\text{Ti, Me}) + \beta(\text{Ti, Me})$ of phase diagrams Ti–Cr, Ti–Co, and Ti–Cu. Temperature dependences of the fraction of grain boundaries $\beta(\text{Ti, Me})/\alpha(\text{Ti, Me})$ completely “wetted” by interlayers of the second solid phase $\alpha(\text{Ti, Me})$ and average contact angle are measured. The results of microstructural investigations showed that the type and concentration of the second component in the alloy strongly affect the formation of equilibrium grain-boundary interlayers. A nonmonotonic temperature dependence of the fraction of grain boundaries completely wetted by interlayers of the second solid phase in the absence of ferromagnet–paramagnet phase transformations in the volume is revealed for the first time.

Keywords: grain boundaries, titanium alloys, wetting

DOI: 10.3103/S106782121603007X

INTRODUCTION

Titanium and its alloys had found wide application in technology due to high mechanical strength retaining at high temperatures, corrosion resistance, heat resistance, specific strength, low density, and other useful properties [1]. Their high cost is in many cases compensated by larger workability, and in many cases they are the only material that can serve to fabricate the equipment or constructions able to operate under severe conditions.

Mechanical and other operational properties of titanium alloys strongly depend on the structure and morphology of constituent phases [2–4]. For example, the $\alpha(\text{Ti})$ phase often forms peculiar “fringes” in two-phase $\alpha(\text{Ti, Me}) + \beta(\text{Ti, Me})$ polycrystals of titanium alloys (Me are alloying elements in titanium) [5–8]. Such fringes of the second phase can substantially affect the properties of titanium and aluminum alloys, in particular, cutting workability [6]; cracks also can form on them during materials failure [8, 9]. We assume that phase morphology in titanium alloys and, in particular, the formation of such fringes can be determined not only by bulk phase transitions [5, 7]

but by grain-boundary phase transformations as well [10, 11].

It is known that the so-called grain-boundary wetting phase transitions can occur in various systems [10, 11]. It was shown for individual grain boundaries (GB) [12, 13] and polycrystals [14, 15] that equilibrium wetting interlayers of the second phase (melt [13, 16]) or second solid phase [15, 17]), which separate grains of the first phase from each other, can form at the GB above certain temperature T_w (the temperature of grain-boundary wetting phase transition).

Such grain-boundary transformations strongly vary both the microstructure and properties of two-phase materials. The formation of thermodynamically equilibrium interlayers of the second phase above T_w varies mechanical properties of the material (it can lead either to material superplasticity and to embrittlement [18]) and affects the diffusion permeability [19], corrosion resistance [20], recrystallization and grain growth [21], electrical resistance of the material [22], etc.

Recently found grain-boundary phase transitions of wetting by the second solid phase are especially important in this sense [14, 17]. This phase transition

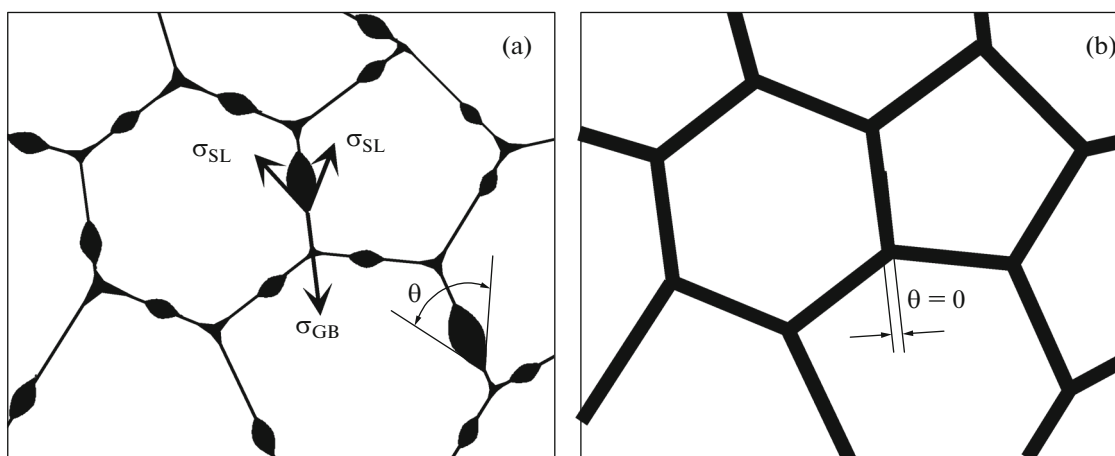


Fig. 1. Schematic image of a polycrystal (a) completely and (b) incompletely wetted with the second phase (the latter is shown black). σ_{GB} and σ_{SL} are free energies of the unit area of surface GBs and liquid–solid interface, respectively. When $2\sigma_{SL}$ becomes smaller than σ_{GB} , then contact angle $\theta = 0$.

can take place in two-phase regions of phase diagrams. The second phase in GBs can have a form of equilibrium thin or thick interlayers (complete wetting) [15, 23] and separate lenslike particles (incomplete wetting) [17, 24] (see schematic image in Fig. 1). The morphology of the second phase is determined by the ratio of GBs and phase interfaces and can depend both on the temperature and on the pressure or concentration of alloying elements [25].

Grain-boundary phase transformation of wetting by the second solid phase (in other words, transitions from equilibrium continuous interlayers on the boundaries to a particle chain with varying the temperature) have already been observed in zirconium–niobium alloys [18], the phase diagram of which is similar to those of titanium alloys with β stabilizers [26]. Therefore, we can expect that such transitions can also occur in titanium alloys.

The search for grain-boundary wetting phase transformations by the second phase in model titanium alloys with chromium, cobalt, and copper is the goal of our study.

EXPERIMENTAL

Titanium alloys with chromium (2, 4, and 5.5 wt %), cobalt (2 and 4 wt %), and copper (2 and 3 wt %) were prepared from high-purity components (4N Ti, 4N Cr, 4N Co, and 4N Cu) by vacuum induction melting. Three-millimeter-thick wafers 10 mm in diameter were cut from fabricated rods. Then polycrystalline samples were sealed into quartz ampules (residual pressure $P = 4 \times 10^{-4}$ Pa) and annealed in a two-phase region $\alpha(\text{Ti,Me}) + \beta(\text{Ti,Me})$ of phase diagrams Ti–Cr, Ti–Co, and Ti–Cu [26] in a temperature range of 600–850°C for 720–860 h. After quenching

into water, the microstructure of the samples under study was investigated with the help of optical and scanning electron microscopy (SEM) using a Tescan Vega TS5130 MM Oxford Instruments scanning microscope, which allows us to perform the phase analysis, and a Neophot-32 optical microscope with a 10 Mpix Canon Digital Rebel XT camera.

The quantitative analysis of the wetting phase transition was performed based on the following criteria:

(i) we assumed that the grain boundary $\beta(\text{Ti,Me})/\beta(\text{Ti,Me})$ is completely wetted by the second solid phase $\alpha(\text{Ti,Me})$ only when the interlayer of the $\alpha(\text{Ti,Me})$ phase completely overlapped the grain boundary;

(ii) the grain boundary considered partially wetted if this interlayer interrupted (see scheme in Fig. 1).

The annealing duration was selected in such a way that the fraction of boundaries completely wetted with the second solid phase would attain the constant value and further would not vary. We analyzed no less than 100 GBs for each annealing temperature.

RESULTS AND DISCUSSION

Figure 2 shows optical micrographs of alloy Ti–4 wt % Cu in the initial cast state and after annealing and quenching. Light areas in all images represent the $\alpha(\text{Ti,Me})$ cubic phase, where Me is Cr, Co, or Cu. The difference in contrast of optical micrographs is associated with the fact that the $\alpha(\text{Ti,Me})$ phase is not subjected to phase transformations upon cooling to room temperature and, therefore, remains lighter after metallographic etching. The fraction of completely wetted GBs (at least 100 GBs) were counted by a series of micrographs made for each annealing temperature.

Figure 3 shows SEM images of the Ti–4 wt % Co alloy annealed at $t = 720^\circ\text{C}$ for $\tau = 720$ h and results of measuring the cobalt concentration along the line intersecting the grain boundary $\beta(\text{Ti},\text{Co})/\beta(\text{Ti},\text{Co})$. In contrast with optical micrographs presented in Fig. 2, contrast in the image is determined by various contents of cobalt in titanium rather than by the result of metallographic etching in this case. Therefore, the $\alpha(\text{Ti},\text{Co})$ phase looks darker than the $\beta(\text{Ti},\text{Co})$ phase in Fig. 3a (in contrast to the structures shown in Fig. 2).

According to the phase diagram of the Ti–Co system, the $\alpha(\text{Ti},\text{Co})$ phase should contain about 0.5 wt % Co at $t = 720^\circ\text{C}$, while the $\beta(\text{Ti},\text{Co})$ phase should contain about 5 wt % Co, respectively [26]. Just these concentrations are observed in the profile presented in Fig. 3b.

Figure 3a shows the $\beta(\text{Ti},\text{Co})/\beta(\text{Ti},\text{Co})$ GB, on which a continuous interlayer of the $\alpha(\text{Ti},\text{Co})$ phase is arranged. In other words, this GB is completely wetted by the $\alpha(\text{Ti},\text{Co})$ second solid phase, while the concentration profile in Fig. 3b intersects this GB.

Figure 4 represents the results of measurements of contact angles and the fraction of the $\beta(\text{Ti},\text{Co})/\beta(\text{Ti},\text{Co})$ GBs completely wetted with the $\alpha(\text{Ti},\text{Co})$ second solid phase.

Let us consider the titanium–cobalt system in more detail. Figure 4b shows two temperature dependences of the fraction of completely wetted GBs and average contact angle. The GB fractions initially rise with an increase in the annealing temperature for both studied alloys, while the values of the average contact angle drop and tend to zero. On the contrary, the fraction of completely wetted GBs at above $\sim 750^\circ\text{C}$ drops with an increase in t , while the value of θ rises. Here-with, the amount of the $\alpha(\text{Ti},\text{Co})$ wetting phase decreases because of approaching the boundary of the $\alpha(\text{Ti},\text{Co}) + \beta(\text{Ti},\text{Co})$ two-phase region with a single-phase $\beta(\text{Ti},\text{Co})$ one. Due to this, both dependences have the clearly pronounced maximum at $t \sim 750^\circ\text{C}$.

A maximum of the fraction of the $\beta(\text{Ti},\text{Co})/\beta(\text{Ti},\text{Co})$ GBs completely wetted by the $\alpha(\text{Ti},\text{Co})$ solid phase is also observed for titanium–chromium alloys in the temperature dependence (see Fig. 4a), and its temperature shifts from 670°C to 820°C through 730°C with a decrease in the chromium concentration from 5.5 to 2 wt %; i.e., the higher the concentration is, the lower the wetting transition temperature is.

An increase in the fraction of completely wetted boundaries is observed in the titanium–copper system (see Fig. 4c) with an increase in temperature up to its magnitude, where the $\alpha(\text{Ti},\text{Cu}) + \beta(\text{Ti},\text{Cu})$ two-phase region transforms into the $\beta(\text{Ti},\text{Cu})$ single-phase one [26].

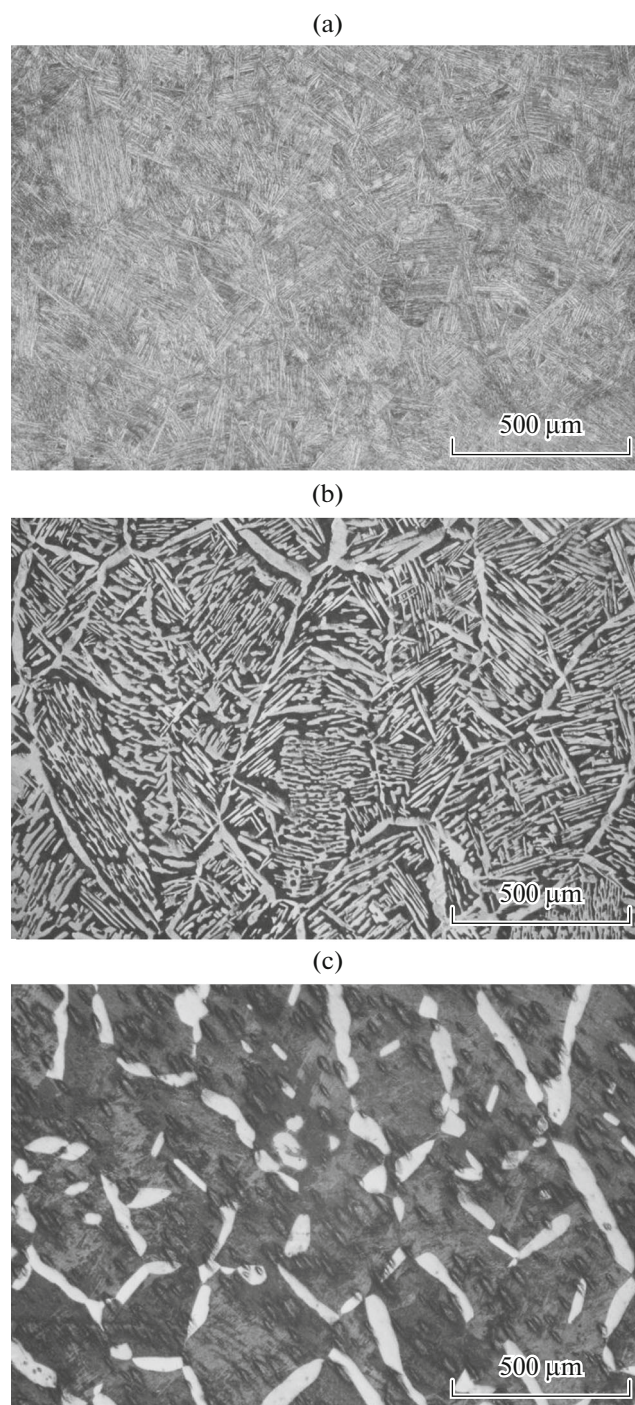


Fig. 2. Optical micrographs of the Ti–4 wt % Co alloy. (a) Initial cast alloy, (b) alloy annealed at $t = 690^\circ\text{C}$ ($\tau = 720$ h), and (c) alloy annealed at 780°C (780 h).

Thus, a double phase transition of GBs wetting by the second solid phase occurs in titanium–cobalt and titanium–chromium alloys, while the fraction of completely wetted GBs depends nonmonotonically on t in a range from the eutectoid temperature to the temperature of α – β transformation in pure titanium.

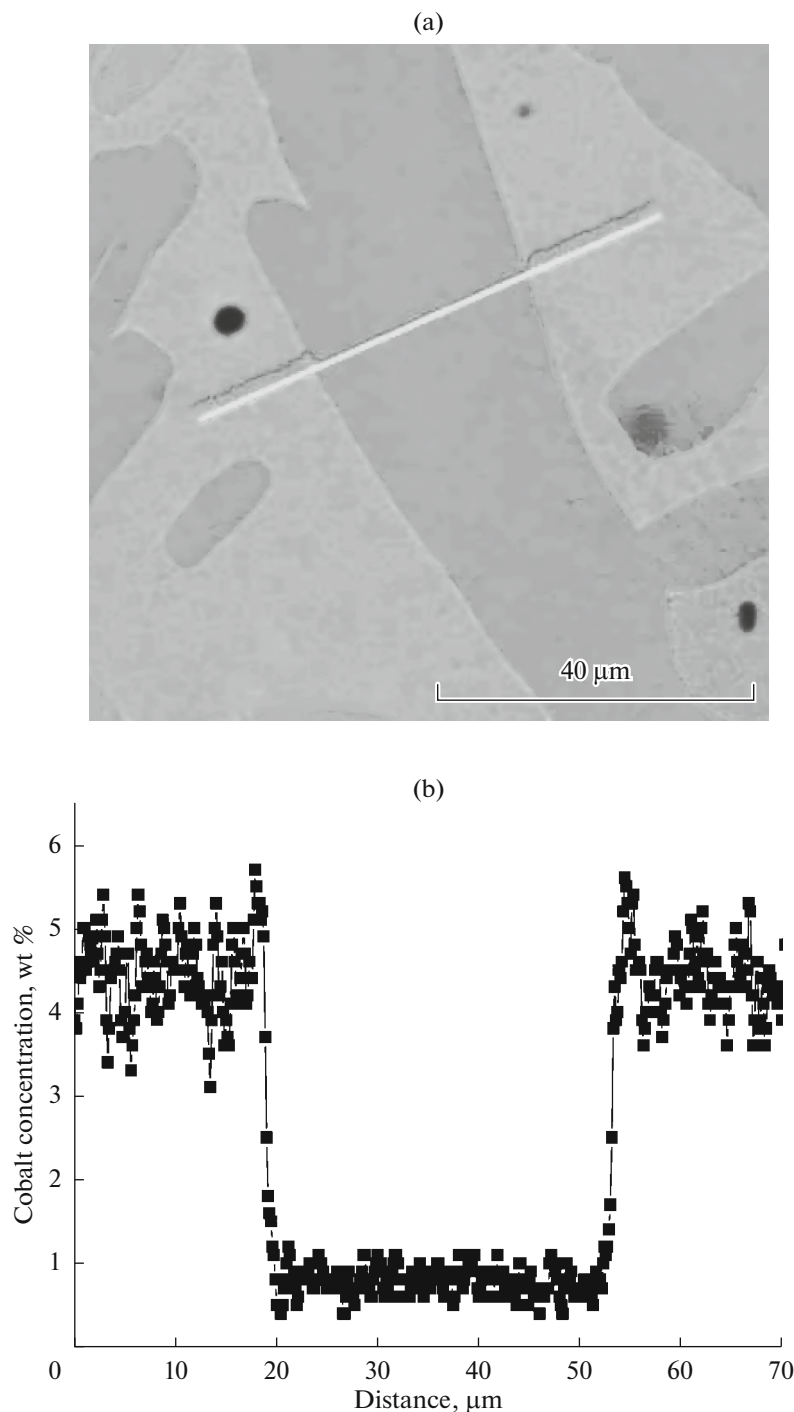


Fig. 3. (a) SEM image with a scanning line across the $\beta(\text{Ti},\text{Co})/\beta(\text{Ti},\text{Co})$ GB and (b) concentration profile recorded along this line in the Ti–4 wt % Co alloy annealed at $t = 720^\circ\text{C}$ ($\tau = 720$ h).

Incomplete wetting is switched to complete one upon increasing t , and then becomes incomplete again. Such a transformation was for the first time observed in a system where there are no additional second-order phase transitions in the bulk (for example, ferromagnet–paramagnet transformations), which can affect the shape of

temperature dependences of free energies of GBs and phase interfaces. This is referred to a temperature range from the eutectoid temperature to the temperature of the α – β transformation in pure titanium.

What can be the cause of a double-phase transition of wetting GBs by a second solid phase (from incom-

plete to complete wetting upon increasing the temperature and back to incomplete wetting)? If the wetting phase is liquid, then its free energy always decreases more rapidly with an increase in temperature than the free energy of the solid phase (because of the higher entropy of a liquid phase), and temperature dependences of free energies $2\sigma_{SL}$ and σ_{GB} intersect only once. On the contrary, if both phases (matrix and wetting ones) are solid, then the corresponding temperature dependences of free energies can intersect twice and incomplete wetting can change to complete wetting upon increasing the temperature and come to incomplete wetting again.

Thus, it is established experimentally that the equilibrium morphology of the $\alpha(\text{Ti,Me})$ phase over the $\beta(\text{Ti,Me})/\beta(\text{Ti,Me})$ GBs can vary reversibly with temperature, and the $\alpha(\text{Ti,Me})$ phase can form both continuous interlayers and particle chains along $\beta(\text{Ti,Me})/\beta(\text{Ti,Me})$ GBs. Continuous $\alpha(\text{Ti,Me})$ interlayers correspond to complete wetting, while particle chains with a nonzero contact angle (see Fig. 1a) correspond to incomplete wetting of the $\beta(\text{Ti,Me})/\beta(\text{Ti,Me})$ GBs by the second solid phase.

Our results allow us to newly interpret, for example, the facts of formation of the so-called fringes of the $\alpha(\text{Ti,Me})$ phase along the boundaries of initial $\beta(\text{Ti,Me})$ grains after various types of thermal and/or thermomechanical treatment of titanium alloys known for a long time [27–29]. For example, the morphology of GB interlayers in VT23 alloy varies after repeated heating by the electron beam and substantially affects the mechanical properties of weld seams [27].

We can also observe the correlation of the morphology of GB interlayers in VT23 alloy with its elasticity moduli [28]. Thermocycling of large billets of VT23 alloy makes it possible to improve their plasticity and impact toughness [29]. This occurs, in particular, due to the division of continuous extended plates of the $\alpha(\text{Ti,Me})$ phase and their subsequent spheroidization. In other words, the transition from complete GB wetting to incomplete wetting is used in this technology.

Further, the observed morphological variation of the $\alpha(\text{Ti,Me})$ phase in VT6 alloy at various hydrogen concentrations [30] can be also interpreted as the manifestation of the transition from complete to incomplete wetting of $\beta(\text{Ti,Me})/\beta(\text{Ti,Me})$ GBs by the $\alpha(\text{Ti,Me})$ second solid phase. Such morphological phase variation in turn affects the fatigue properties of VT6 alloy [30]. Particle chains and continuous interlayers of the $\alpha(\text{Ti,Me})$ phase are clearly distinguishable at $\beta(\text{Ti,Me})/\beta(\text{Ti,Me})$ GBs and in VT5-1kt titanium alloy fabricated by compacting the hydrogenated granules [31].

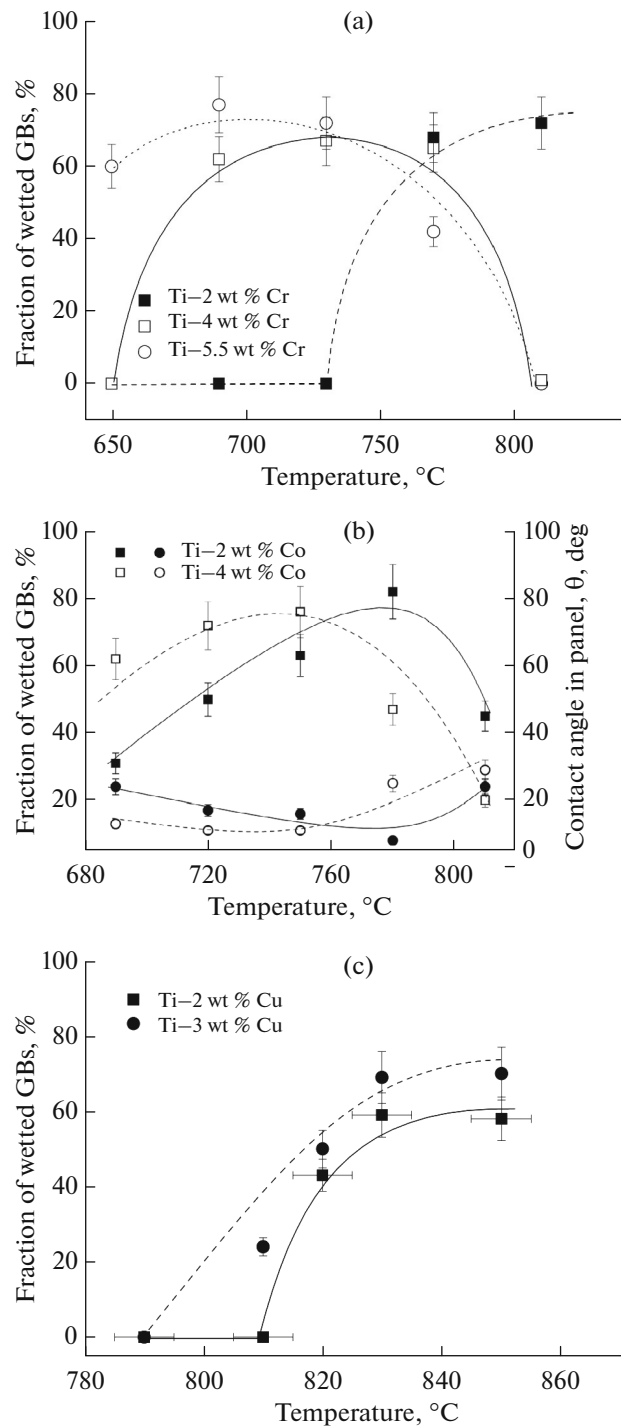


Fig. 4. Temperature dependences for the fraction of completely wetted GBs in alloys (a) Ti–Cr, (b) Ti–Co, and (c) Ti–Cu, as well as for the average contact angle in the Ti–Co alloy.

CONCLUSIONS

(i) Complete or incomplete wetting the $\beta(\text{Ti,Me})/\beta(\text{Ti,Me})$ GBs by interlayers of the $\alpha(\text{Ti,Me})$ second phase was found for all studied Ti–Me binary alloys (where Me is Cr, Co, or Cu).

(ii) It is found that the fraction of GBs completely covered by a continuous layer of the α (Ti,Me) phase is nonmonotonically temperature-dependent in a range from the eutectoid temperature to the temperature of the α – β transformation in pure titanium.

(iii) Such a transformation was observed for the first time in a system where there is no additional second-order phase transitions in the bulk (for example, ferromagnet–paramagnet phase transformations), which can affect the shape of temperature dependences of free energies of GBs and phase interfaces (this is referred to a temperature range from the eutectoid one to the temperature of the α – β transformation in pure titanium).

ACKNOWLEDGMENTS

This study was supported by the Russian Foundation for Basic Research, project nos. 12-03-00894, 16-53-12007, and 15-53-06008; the German Research Society (DFG); and the Ministry of Science, Technology, and Space of Israel.

REFERENCES

- Il'in, A.A., Kolachev, B.A., and Pol'kin, I.S., *Titanovye splavy. Sostav, struktura, svoystva* (Titanium Alloys. Composition, Structure, and Properties), Moscow: Vseross. Inst. Legk. Splavov–Mosk. Aviats. Tekhnol. Inst., 2009.
- Kolachev, B.A., *Fizicheskoe metallovedenie titana* (Physical Metallurgy of Titanium), Moscow: Metallurgiya, 1976.
- Kolachev, B.A., Yeliseev, Yu.S., Bratukhin, A.G., and Talalaev, V.D., *Titanovye splavy v konstruktivnykh i proizvodstve aviadvigatelei i aviatsionno-kosmicheskoi tekhnike* (Titanium Alloys in Constructions and Production of Aircraft Engines and Aerospace Engineering), Moscow: Moscow Aviats. Inst., 2001.
- Kolachev, B.A., Betsofen, S.Ya., Bunin, L.A., and Volodin, V.A., *Fiziko-mekhanicheskie svoystva legkikh konstruktivnykh splavov* (Physicomechanical Properties of Light Construction Alloys), Moscow: Metallurgiya, 1995.
- Kolachev, B.A. and Lyasotskaya, V.S., Correlation between diagrams of isothermal and anisothermal transformations and phase state diagrams of hardened titanium alloys, *Met. Sci. Heat Treat.*, 2003, vol. 45, pp. 119–126.
- Egorova, Yu.B., Il'in, A.A., Kolachev, V.A., Nosov, V.K., and Mamonov, A.M., Influence of structure on cutting workability of titanium alloys, *Met. Sci. Heat Treat.*, 2003, vol. 45, pp. 134–139.
- Kolachev, B.A., Veitsman, M.G., and Gus'kova, L.N., Structure and mechanical properties of annealed titanium alloys, *Met. Sci. Heat Treat.*, 1983, pp. vol. 25, pp. 626–631.
- Fishgoit, A.V., Maistrov, V.M., and Rozanov, M.A., Interaction of short cracks with the structure of metals, *Sov. Mater. Sci.*, 1988, vol. 24, pp. 247–251.
- Bobovnikov, V.N., Luk'yanenko, V.V., and Fishgoit, A.V., Effect of particles of the insoluble phase Al_9FeNi on the kinetics of fatigue crack propagation in alloy AK4-1, *Met. Sci. Heat Treat.*, 1982, vol. 24, pp. 191–194.
- Straumal, B.B., Gust, W., and Watanabe, T., Tie lines of the grain boundary wetting phase transition in the Zn-rich part of the Zn–Sn phase diagram, *Mater. Sci. Forum*, 1999, vol. 294/296, pp. 411–414.
- Straumal, B.B., Baretzky, B., Kogtenkova, O.A., Straumal, A.B., and Sidorenko, A.S., Wetting of grain boundaries in Al by the solid Al_3Mg_2 solid phase, *J. Mater. Sci.*, 2010, vol. 45, 2057–2061.
- Semenov, V.N., Straumal, B.B., Glebovsky, V.G., and Gust, W., Preparation of Fe–Si single crystals and bicrystals for diffusion experiments by the electron-beam floating zone technique, *J. Crystal Growth*, 1995, vol. 151, pp. 180–186.
- Gornakova, A.S., Straumal, B.B., Tsurekawa, S., Chang, L.-S., and Nekrasov, A.N., Grain boundary wetting phase transformations in the Zn–Sn and Zn–In systems, *Rev. Adv. Mater. Sci.*, 2009, vol. 21, pp. 18–26.
- Straumal, B.B., Gornakova, A.S., Kucheev, Y.O., Baretzky, B., and Nekrasov, A.N., Grain boundary wetting by a second solid phase in the Zr–Nb alloys, *J. Mater. Eng. Perform.*, 2012, vol. 21, pp. 721–724.
- Straumal, B.B., Kucheev, Y.O., Efron, L.I., and Petelin, A.L., Dutta Majumdar, J., and Manna, I., Complete and incomplete wetting of ferrite grain boundaries by austenite in the low-alloyed ferritic steel, *J. Mater. Eng. Perform.*, 2012, vol. 21, pp. 667–670.
- Straumal, B.B., Gornakova, A.S., Kogtenkova, O.A., Protasova, S.G., Sursaeva, V.G., and Baretzky, B., Continuous and discontinuous grain boundary wetting in the Zn–Al system, *Phys. Rev. B*, 2008, vol. 78, p. 054202.
- Gornakova, A.S., Straumal, B.B., Petelin, A.L., and Straumal, A.B., Solid-phase wetting at grain boundaries in the Zr–Nb system, *Bull. Russ. Acad. Sci. Phys.*, 2012, vol. 76, pp. 102–105.
- Straumal, B.B., Gornakova, A.S., Mazilkin, A.A., Fabrichnaya, O.B., Kriegel, M.J., Baretzky, B., Jiang, J.-Z., and Dobatkin, S.V., Phase transformations in the severely plastically deformed Zr–Nb alloys, *Mater. Lett.*, 2012, vol. 81, pp. 225–228.
- Noskovich, O.I., Rabkin, E.I., Semenov, V.N., and Straumal, B.B., The zinc penetration along tilt grain boundary $38^\circ[100]$ in Fe–12 at % Si alloy near ordering A2–B2 in the bulk, *Scr. Metall.*, 1991, vol. 25, pp. 1441–1446.
- Baretzky, B., Baró, M.D., Grabovetskaya, G.P., Gubicza, J., Ivanov, M.B., Kolobov, Yu.R., Langdon, T.G., Lendvai, J., Lipnitskii, A.G., Mazilkin, A.A., Nazarov, A.A., Nogués, J., Ovidko, I.A., Protasova, S.G., Raab, G.I., Révész, A., Skiba, N.V., Sort, J., Starink, M.J., Straumal, B.B., Suriñach, S., Ungár, T., and Zhilyaev, A.P., Fundamentals of interface phenomena in advanced bulk nanoscale materials, *Rev. Adv. Mater. Sci.*, 2005, vol. 9, pp. 45–108.
- Sursaeva, V., Straumal, B., Risser, S., Chenal, B., Gust, W., and Shvindlerman, L., Orientation relationships between grains and grain boundaries in Al–1 wt %

- Ga alloy at the beginning of secondary recrystallization, *Phys. Stat. Sol. A*, 1995, vol. 149, pp. 379–387.
22. Straumal, B., Sluchanko, N.E., and Gust, W., Influence of grain boundary phase transitions on the properties of Cu–Bi polycrystals, *Def. Diff. Forum*, 2001, vol. 188–190, pp. 185–194.
 23. Straumal, B., Gust, W., and Molodov, D., Wetting transition on the grain boundaries in Al contacting with Sn-rich melt, *Interface Sci.*, 1995, vol. 3, pp. 127–132.
 24. Straumal, B.B., Kogtenkova, O.A., Straumal, A.B., Kucheyev, Yu.O., and Baretsky, B., Contact angles by the solid-phase grain boundary wetting in the Co–Cu system, *J. Mater. Sci.*, 2010, vol. 45, pp. 4271–4275.
 25. Straumal, B., Rabkin, E., Lojkowski, W., Gust, W., and Shvindlerman, L.S., Pressure influence on the grain boundary wetting phase transition in Fe–Si alloys, *Acta Mater.*, 1997, vol. 45, pp. 1931–1940.
 26. *Binary Alloy Phase Diagrams*, Massalski, T.V., Ed., Materials Park, OH: ASM, 1980.
 27. Lyasotskaya, V.S., Knayzeva, S.I., and Lysenkov, Yu.T., Mechanical properties of welded joints of alloy VT23 after repeated heating by an electron beam, *Met. Sci. Heat Treat.*, 1995, vol. 37, pp. 349–352.
 28. Lyasotskaya, V.S., Fedotov, S.G., Knyazeva, S.I., and Dmitriev, A.A., Phase composition and elastic moduli of the titanium alloy VT23, *Met. Sci. Heat Treat.*, 1993, vol. 35, pp. 242–246.
 29. Lyasotskaya, V.S., Khorev, A.I., Sergeev, K.N., Khyazeva, S.I., and Gorbunova, I.L., Improvement in the properties of alloy VT23 large semifinished products by thermal cycling treatments, *Met. Sci. Heat Treat.*, 1992, vol. 24, pp. 70–73.
 30. Mal'kov, A.V., Kolachev, B.A., Mishanova, M.G., and Bylov, B.B., Effect of hydrogen on fatigue of VT6 alloy, *Strength Mater.*, 1984, vol. 16, pp. 385–389.
 31. Shevchenko, V.V., Nizkin, I.D., Mal'kov, A.V., and Luk'yanova, E.V., Features of compacting hydrogen-doped granules in a VT5-1kt titanium alloy, *Russ. J. Non-Ferrous Met.*, 2008, vol. 49, pp. 181–186.

Translated by N. Korovin